

Design, manufacture and experimental verification of side safety device of Wielton trucks

Projektowanie, wytwarzanie i badania weryfikacyjne bocznego urządzenia zabezpieczającego do pojazdów ciężarowych Wielton

MARIAN KLASZTORNY
ARKADIUSZ CZARNUCH
ROMAN ROMANOWSKI
DANIEL B. NY CZ
MARIUSZ GOLEC
MACIEJ KACZOR *

DOI: <https://doi.org/10/17814/mechanik.2017.2.33>

The study presents a new design-technological solution of a side safety device for Wielton trucks. A side safety device is manufactured of glass-polyester laminates and foam using press technology. Numerical modelling in MSC.Marc system and experimental validation tests were conducted according to Regulations no. 73. A good qualitative and quantitative compatibility of the results, were obtained.

KEYWORDS: side safety device, manufacture, numerical modelling, validation experimental tests

Side safety device (SSD) on trucks is used to protect bikers from falling into the vehicle in case of an accident/collision. SSD, commonly known as anti-roll or antiwear protector, is an element of truck/trailer equipment. On the market, this device is offered mostly in the form of prismatic, closed thin-walled aluminum profiles, one- or two-box, for which individual screw joints should be designed depending on the type of semi-trailer/trailer (e.g. www.autoakcesoria.com.pl/sklep/zderzaki). Hot dip galvanized steel covers and EPDM overlays are also offered.

Wielton S.A. in co-operation with Roma Ltd. and Military University of Technology, Warsaw have designed a new type of composite SSD for Wielton trucks. This paper presents results of the design, fabrication and verification tests this bump.

SSD design project

SSD for Wielton semitrailers/trailers is a polyester-glass composite body with an original industrial design, taking into account safety, load capacity, usability, assembly and aesthetics.

Figure 1 shows the final, dimensioned SSD construction drawings, except for the thicknesses of the

composite shells being the design parameter. A back composite rib with foam insert was designed at the interval between the embossings. The foam insert has a trapezoidal cross-section. On the CNC machine, one can cut the concave tips of the foam insert so that there are no clearances between the embossing and the insert. Approved total thickness of 40 mm was accepted.

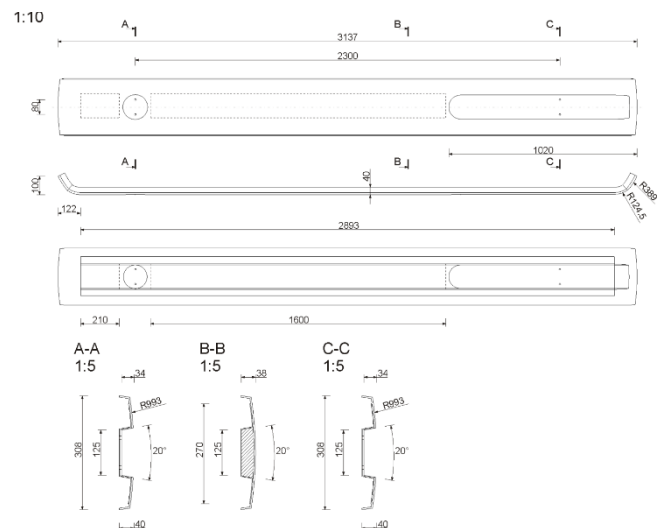


Fig. 1. Structural design of SSD for Wielton trailer/ semitrailer

Production of SSD segments

The SSD trial series was manufactured at Roma Ltd. in Grabowiec (www.roma.torun.pl), specializing in modern technologies and production of polyester-glass composite structures.

Pressing technology is used in SSD production. The rigid, lockable composite mold consists of a bottom mold (on front side of the bump) and a top mold (on the back side of the bump). When applied to the surface of both forms of release agents, in the bottom form, decorative, anti-osmotic, UV resistant, with increased flexibility layer is applied. The layers of glass reinforcement and foam core are applied to the decorative layer. The reinforcement layers, adequately stacked for extrusion, are pre-poured with polyester resin. Then the mold is closed with the top cover. At a pressure of 4 bar and at 24 °C, the mold is closed. During slow closing (taking

* Prof. dr hab. inż. Marian Klasztorny (m.klasztorny@gmail.com) – Wydział Mechaniczny Wojskowej Akademii Technicznej; lic. Roman Romanowski (rromanowski@roma.torun.pl) – Roma Sp. z o.o.; dr inż. Daniel B. Nycz (daniel.nycz@interia.pl) – Państwowa Wyższa Szkoła Zawodowa, Sanok; inż. Arkadiusz Czarnuch (a.czarnuch@wielton.com.pl), inż. Mariusz Golec (m.golec@wielton.com.pl), inż. Maciej Kaczor (m.kaczor@wielton.com.pl) – Wielton S.A., Wieluń

into account resin parameters, i.e. gelling time and curing time), the glass reinforcement is saturated and the excess resin extruded.

Numerical modeling and SSD test loads

The geometric model of the bump was created in the Catia v5 environment. Simplification of the geometry to mid-surfaces and FEM meshing was done using Altair HyperMesh 12.0 software. The average mesh size of finite elements was equal to 10 mm. The total number of finite elements was 15,863 (number of nodes 15,978). Figure 2 shows a meshed model of the bump in the isometric view at the front. In the calculations, the foam filling, which is used for technological purposes and serves only to produce the rear rib, is omitted.

The QUAD4 (15 841 elements) and TRIA 3 (22 elements) finite elements were assigned with Bilinear Thick-shell Element [1]. Layers of laminates were assigned with an orthotropic material model of linear elastic-brittle with the criterion of progressive destruction of Hashin-Fabric [2]. Basic material constants of the laminates are listed in Table I. Directions 1 and 2 are directions of the warp and weft yarns, and direction 3 is the direction of the lamina thickness.

Static calculations used material constants and laminates corresponding to manual technology and temperature of 20 °C. Due to the application of press technology, the degree of reinforcement of the laminate was changed, i.e. the amount of resin decreases (reduction of laminate thickness). On the basis of preliminary calculations, the increase in deflection of the bump and effort index of the press was estimated to be approximately 10% as compared to the manual bump.

The SSD test load are specified in Regulation 73 [3]. The bump was loaded with a perfectly rigid cylindrical punch of $\varnothing 220$ mm in force, in two variants illustrated in Figures 3 and 4 (variant 1 - middle load, variant 2 - side load). Between the punch and the bump, a Tauching contact model based on the Constrain Method [2] was defined, with a friction coefficient of 0.29 (friction pair: composite - steel [4]).

For variant 1, the loading force $F_0 = 1000$ N acts in the middle of the span of the bump. Acceptable deflection $w_{dop} = 150$ mm [3], and the acceptable value of laminate effort index $R_{dop} = 0.60$. For variant 2, the loading force $F_0 = 1000$ N acts on the extreme part of the bump. Acceptable deflection $w_{dop} = 30$ mm [3], and the acceptable value of laminate effort index $R_{dop} = 0.60$.



Fig. 2. SSD meshed model - isometric view at the front

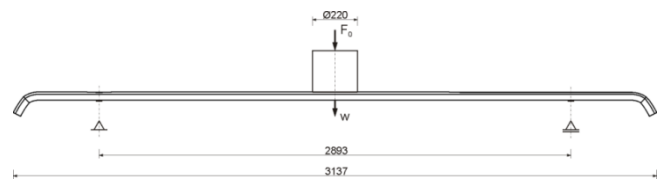


Fig. 3. Variant 1 of the SSD load (centre position)

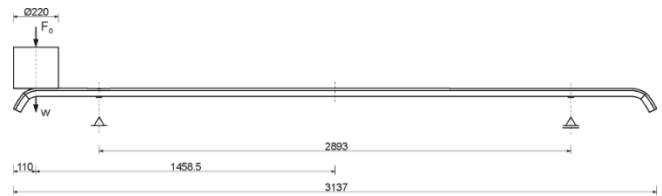


Fig. 4. Variant 1 of the SSD load (side position)

TABLE I. Basic elastic and strength constants of glass-polyester laminates reinforced with fabric or mat at 20 °C [4]

Type of laminate	Glass-polyester composite reinforced with fabric	Glass-polyester composite reinforced with mat
Young's module in direction 1 at stretching E_{11} , GPa	16,9	8,46
Young's module in direction 1 under compression E_{1c} , GPa	18,5	9,41
Poisson's ratio in plane 12 ν_{12}	0,15	0,40
Shear module (Kirchhoff) in plane 12 G_{12} , GPa	2,43	2,79
Shear module (Kirchhoff) in plane 13 G_{13} , GPa	0,564	0,989
Tensile strength in direction 1 R_{1t} , MPa	279	99,0
Compression strength in direction 1 R_{1c} , MPa	203	221
Shear strength in plane 12 (standard) R_{12} , MPa	34,5	87,9
Shear strength in plane 13 R_{13} , MPa	23,0	34,7

The screw connections on the brackets were modelled as articulated joints, not movable on one side and sliding on the other side of the bump.

Laminate design consisted of performing static calculations for five ply sequences (2 to 4 layers for front laminate, 1 to 3 layers for rear laminate, reinforcement: glass plain weave fabric, glass mat). The studied laminate systems and the final system are the industrial property of Roma.

Static calculations were performed using MSC.Marc finite element code [2]. The Newton-Raphson method was used with the force and displacement criterion of convergence [2].

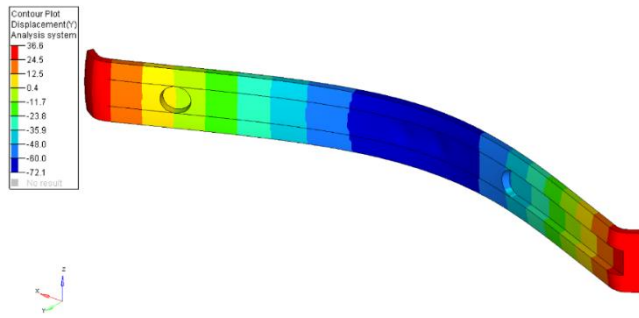


Fig. 5. Displacement contour map towards force and SSD deformation (deformation scale 5:1) - load variant 1, variant S05 of laminate ply sequence

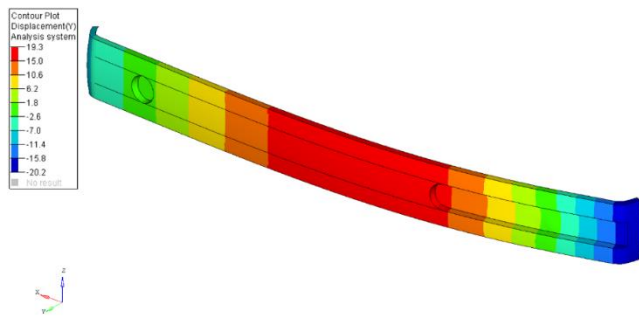


Fig. 6. Displacement contour map towards deformation and SSD deformation (deformation scale 5:1) - load variant 2, variant S05 of laminate ply sequence

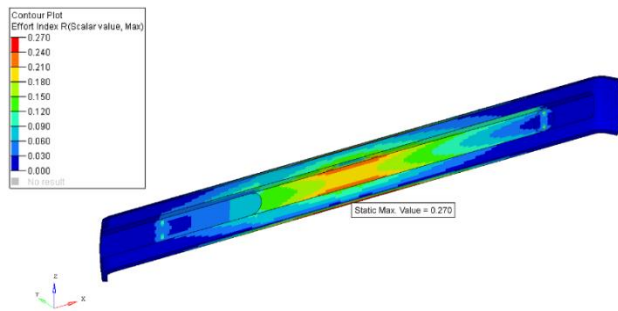


Fig. 7. Effort index R contour map of the SSD device - load variant 1, variant S05 of the laminate ply sequence

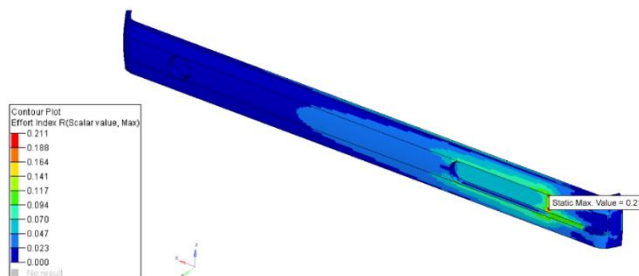


Fig. 8. Effort index R contour map of the SSD device - load variant 2, variant S05 of the laminate ply sequence

Results of SSD static calculations

Figures 5 and 6 show the displacement contour maps in the direction of forcing and deformation of the SSD on the test bench (scale 5:1) for ply sequence S05, recommended for the production of press-molding technology. Figures 7 and 8 illustrate contour maps of R-indexes (through all layers and all Hashin-Fabric failure

modes) for the sequence of layers of laminates S05. In Table II, the numerical predicted values of the vertical displacement of the bump (under the stamp load) and the values of the effort index corresponding to the five variants of the laminate layers of the front and rear laminates are presented.

TABLE II. Predicted numerical values of vertical displacement of SSD on test bench (under load stamp) and values of effort index R, corresponding to five variants of the front and rear laminate layouts

Ply sequence variant	Load variant	Limit values		w, mm	R
		w _v , mm	R _v		
S01	1	150	0,60	26,8	0,128
	2	30	0,60	5,6	0,082
S02	1	150	0,60	41,3	0,164
	2	30	0,60	7,5	0,119
S03	1	150	0,60	87,5	0,333
	2	30	0,60	14,4	0,271
S04	1	150	0,60	61,4	0,230
	2	30	0,60	10,4	0,179
S05	1	150	0,60	71,7	0,270
	2	30	0,60	12,0	0,211

Experimental SSD tests

The experimental tests (validation) of the SSD designed to meet homologation requirements under Regulation 73 [3] were carried out in August 2016 in Wielton in Wieluń (www.wielton.com.pl).

Segments were supplied by the manufacturer - Roma in Grabowiec - in two versions, i.e. S05 and S04, differing in the laminate reinforcement. In variant S04, the thickness of laminates is 30% higher than in variant S05.

A test stand (fig. 9) was built for strength tests of bumps.

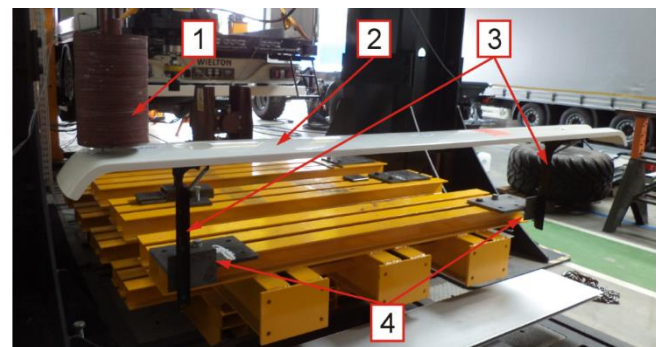


Fig. 9. SSD validation station according to [3], consisting of the following subsystems: 1 - 100 kg cylindrical weight and a diameter of $\varnothing 220$ mm, 2 - tested segment (bump), 3 - supports, 4 - rigid elements replacing the longitudinal beams of the main vehicle (source: Wielton S.A.)

The load was controlled by crane scales. Measurements of deflection of the examined segment were made with a laser rangefinder. The retract was fixed to the supports spaced by 2300 mm using two M8 screws on each support. The experimental conditions were similar to the actual conditions in Wielton vehicles.

According to Ref. [3], the side safety device is considered to be suitable if it is capable of withstanding a static horizontal force of 1 kN, applied perpendicular to any part of its outer surface with a round and flat end with a diameter of $\varnothing 220 \text{ mm} \pm 10 \text{ mm}$, and if the displacement of the device under this load measured in the middle of the punch is not greater than:

- 30 mm on the most rearward section of the device measuring 250 mm,
- 150 mm in the rest of the device.



Fig. 10. SSD load in the extreme front position (source: Wielton S.A.)



Fig. 11. SSD load in the middle position (source: Wielton S.A.)

Profiles - in the two versions provided - were tested in accordance with the guidelines [3]. The tests were carried out by applying the load in the extreme front (fig. 10), in the extreme rear position and in the middle position (fig.11). For each case, the deflection was measured against the original unloaded profile. The results of the measurement of deflections are summarized in Table III.

TABLE III. Results of the measured deflection of tested SSD segments under 100 kg load

Case SP05		Deflection, mm		
		on the front	in the middle	at the back
Load location	on the front	12	–	–
	in the middle	–	66	–
	at the back	–	–	14
Case SP04		Deflection, mm		
		on the front	in the middle	at the back
Load location	on the front	10	–	–
	in the middle	–	58	–
	at the back	–	–	8

Conclusions from the validation experimental studies are as follows:

- Measured displacement was within the elastic range. After removing the load, SSD profile showed a tendency to return to its original shape.
- After the experiments of the SSD profiles, a visual assessment was performed, during which no mechanical damage to the tested segments was observed.
- The relative differences in the results of the simulated deflections relative to the experimental results are, respectively, for S04 and S05: + 6% and + 9% in the middle of the span with the load at the centre of the span and + 4% and 0% at the front of the beam (in the cantilever section) on the front of the beam. The experimental validation of the simulation results is therefore positive.
- After the experimental tests, it is stated that the new construction of the bumper profile in two versions complies with the strength requirements of Regulation 73 [3].

Conclusions

- All variants of the ply sequences (S01, S02, S03, S04 and S05) meet the load-bearing and serviceability conditions.
- The new SSD construction - in both delivered variants - complies with the strength requirements of Regulation 73 [3].
- Because of the thickness of the laminates and good fabrication of the extruded fabrics, SSD was chosen with the S05 ply sequence (almost thinnest laminates among numerically controlled laminates with a relatively low surface density of the laminate reinforcements).
- The selected SSD construction solution is competitive on the market (low weight, corrosion resistance, low price and aesthetic qualities).

The research was funded by Wielton S.A.

REFERENCES

1. Marc 2008 r1, Vol. B. Element Library. MSC.Software Co., Santa Ana, CA, USA.
2. Marc 2008 r1, Vol. A. Theory and User Information. MSC.Software Co., Santa Ana, CA, USA.
3. Regulamin nr 73 Europejskiej Komisji Gospodarczej Organizacji Narodów Zjednoczonych (EKG ONZ) – Jednolite przepisy dotyczące homologacji.
4. Nycz D. „*Modelowanie i badania numeryczne testów zderzeniowych bariery klasy N2-W4-A na łukach dróg*”. Wydawnictwo WAT. Warszawa 2015. ■